CHAPTER 5: Optimisation for Impact

5.1 Introduction

This chapter covers both the modelling aspects of an impact analysis and the definition of the optimisation problem. The analysis for impact is done using the commercial non-linear finite element solver LS-DYNA 970 [26]. The chapter includes results of the single discipline optimisation for impact, covering impact analyses of both 2D and 3D geometries.

5.2 Impact Analysis

This section discusses the methodology adopted for the modelling of the fluid structure interaction in a liquid container. The analyses will simulate the stresses experienced in the baffles of a liquid container when exposed to accelerations typical of an impact. All procedures are fully automated for the purposes of numerical optimisation.

5.2.1 Mesh generation

Although all analyses are performed by LS-DYNA 970, LSTC (the supplier of LS-DYNA) does not currently provide an adequate parametric pre-processor. The available FEM pre-processor for this study is MSC-Patran [12], a dedicated pre-processor intended for use with MSC FEM solvers e.g., Nastran, Marc, Dytran. Patran does however provide an export function that is compatible with simple models for an older version of LS-DYNA, i.e., v930.

The geometries considered will all be solved using three-dimensional models since two-dimensional simplifications of the geometry are not possible with the available methods. Figure 5.1 and Figure 5.2 below show the forms of the 3D and 2D geometries. The mesh consists of two elements types, brick elements and shell

elements. The brick elements are used for the fluid phases (liquid and gas) while the shell elements are used for the walls of the container and the internal baffles. Although the shell elements occupy zero thickness in the model, they will behave according to the user-specified shell thickness. A fill level of 90% is used for all impact analyses. A higher fill level is used because it represents more fluid inertia and in turn induces higher stresses than the lower 70% fill level used in the sloshing analyses.

Figure 5.3 below illustrates the form of the mesh used in the 3D impact analysis. The image is as seen from one end of the container, perpendicular to the baffle surface. The form of the mesh throughout the length of the model remains as seen in this figure. A typical mesh contains approximately 100 000 hexahedral cells.

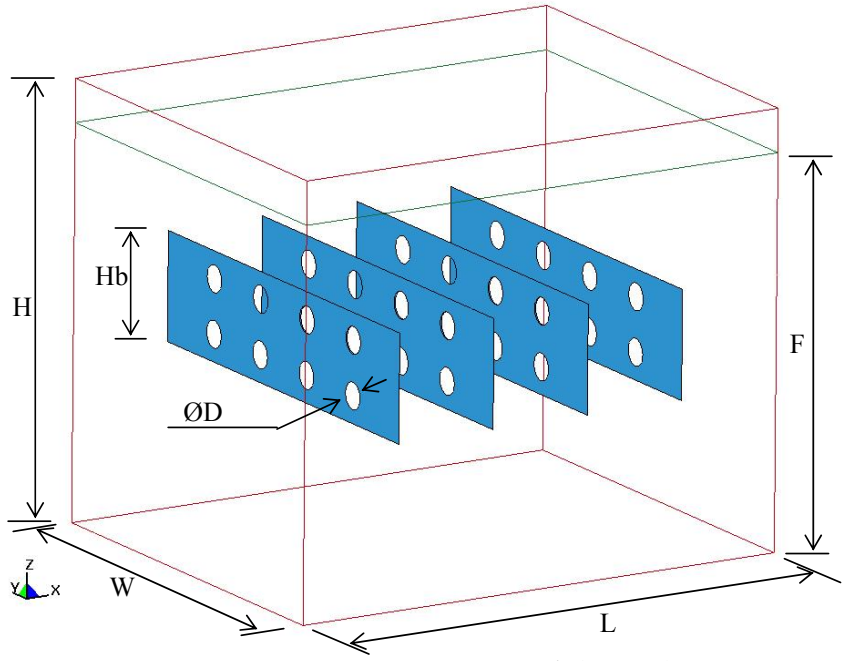

Figure 5.1: Geometry of 3D liquid container

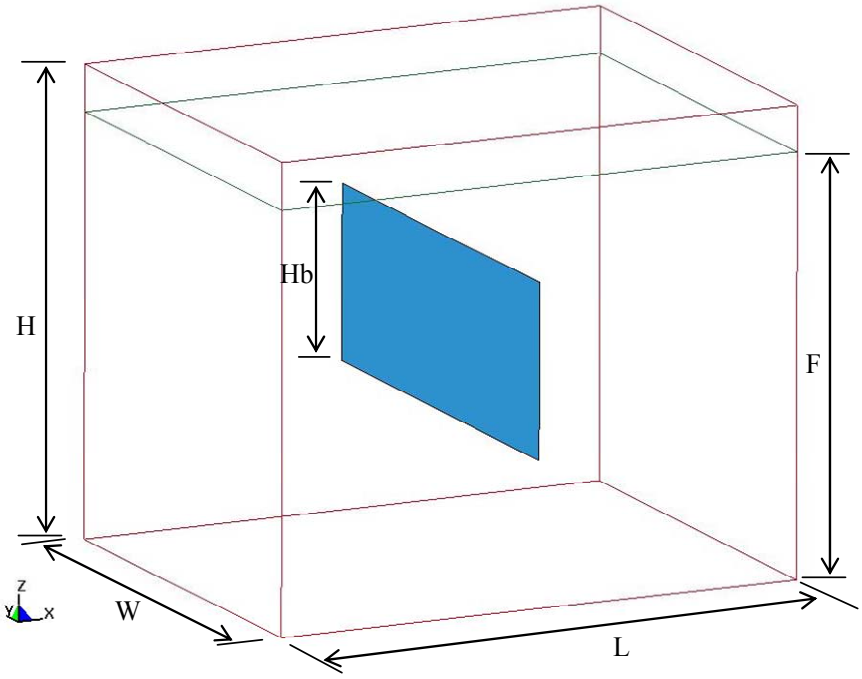

L – Length (500mm)
W – Tank width (400mm)
H – Tank height (400mm)
Hb – Baffle height
F – Fill level (90%)

Figure 5.2: Geometry of 2D "extruded" liquid container

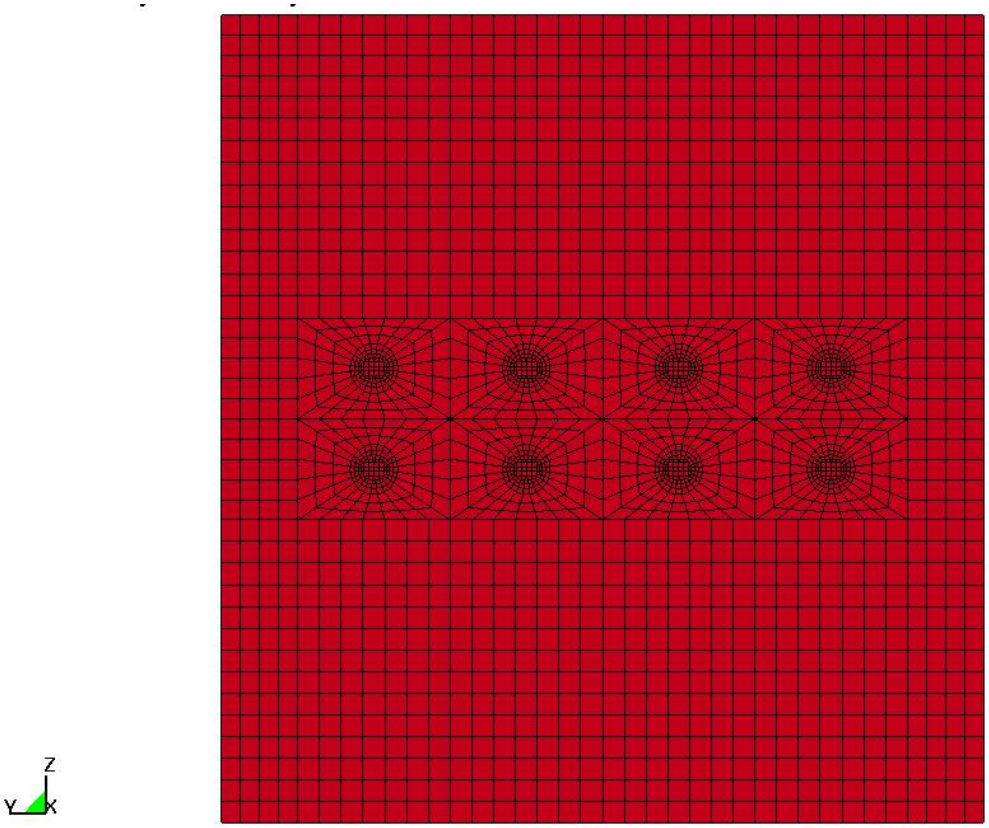

Figure 5.3: Mesh used in LS-DYNA analysis

Since the mesh generation forms part of a typical optimisation procedure, the process needs to be fully automated. As with Gambit before, a text or session file is created that contains a string of command-line commands in Patran Command Language (PCL) that represent Patran actions. By running this session file in batch mode, Patran will generate the mesh according to specified variable values and export the resulting mesh to LS-DYNA v930 format. An example of one such session file can be seen in Appendix S. This file is then cleaned using the scriptable Linux text editor SED that uses a script as seen in Appendix T to remove all but the mesh data.

5.2.2 Model setup

This section describes the setup and assumptions for the impact model. Since LS-DYNA has no graphical user interface in UNIX versions, all settings are loaded to the solver user a text file known as a keyword file. The keyword file contains all models to be included and their corresponding settings, node locations and connectivity data (generated as described above), and the load curves that will be applied during solution.

Since the section of the file that contains the mesh data is generated using Patran, the models and their settings will need to be manually prescribed in the text file. Appendix U provides an example of the section of the keyword that specifies models and model settings. Some of the more significant models used are described below.

The Arbitrary Lagrange-Eulerian (ALE) model is used for cases like the one analysed in this study where fluid motion is modelled in conjunction with structural deformation. Unlike with the Lagrangian formulation, the nodes do not follow the material flow, instead the material flows through a fixed mesh. The structural shell elements are however still treated with the Lagrangian formulation. The ALE model is used together with a fluid-structure coupling algorithm that prescribes the type of interaction that will take place between the materials in the Eulerian mesh and the elements of the Lagrangian structure. In the case of this study a Penalty coupling algorithm is used, as described in section 2.4.4 of this dissertation.

Other significant entries in the keyword file include those that describe the material properties of the various elements used in the analysis. These include the following materials.

The first material type is the rigid material that is used for the walls of the liquid container itself. No stress distribution is solved in these elements. The second material type is the plastic-kinematic material used for the shell elements of the baffles. All stresses and strains are solved in this material and it is allowed to deform plastically according to material type 3 in LS-DYNA [26] that has a bilinear stress-strain curve. Kinematic hardening is used with a tangent modulus of 100 and no strain effects. The third and fourth materials are of type material null, which implies that no stresses or strains are solved for in elements of the material, but the motion of the material is solved for. These materials will be applied to the air and water inside the container respectively. The difference between these two materials is in their respective densities and viscosities. Table 5.1 below provides the properties of the materials used.

Table 5.1: Table of material properties

Density (container) [kg/m^3]	7830
Density (baffles) [kg/m^3]	7830
Young's modulus (baffles) [GPa]	207
Poisson's ratio (baffles)	0.3
Density (air) [kg/m^3]	1.1845
Viscosity (air) [N.s/m^2]	1.84e-5
Density (water) [kg/m^3]	998
Viscosity (water) [N.s/m^2]	0.001

The final entry in the keyword file includes the load curves that are used during the analysis. The most obvious of these is the gravity vector, which is applied to all materials. The second load curve that is applied to the rigid body only, is that which prescribes the motion of the tank during the impact scenario.

For the purposes of this study a condensed version of the impact load curve analysed by Craig, et al. [37] is used in all the impact analyses. Figure 5.4 below shows the

form of the load curve used for the analyses. The various stages of acceleration are due to various parts of a vehicle being crushed. The full load represents the acceleration seen by the vehicle during a typical NHTSA full frontal collision. The compressed signal is shortened by an order of magnitude while its amplitude is increased 4 times. Using this form of compression, analysis results using the compressed signal provide similar peak stresses in the baffles. The reason for using the compressed signal is due to the time required to run a full analysis. A full length load curve analysis will run for approximately 14 hours on a 3GHz P4 Linux workstation while the compressed-signal analysis will run for 2 hours on the same machine. When considering numerical optimisation on single-processor machines, within the context of this study, it is impractical to wait 14 hours for a single solution.

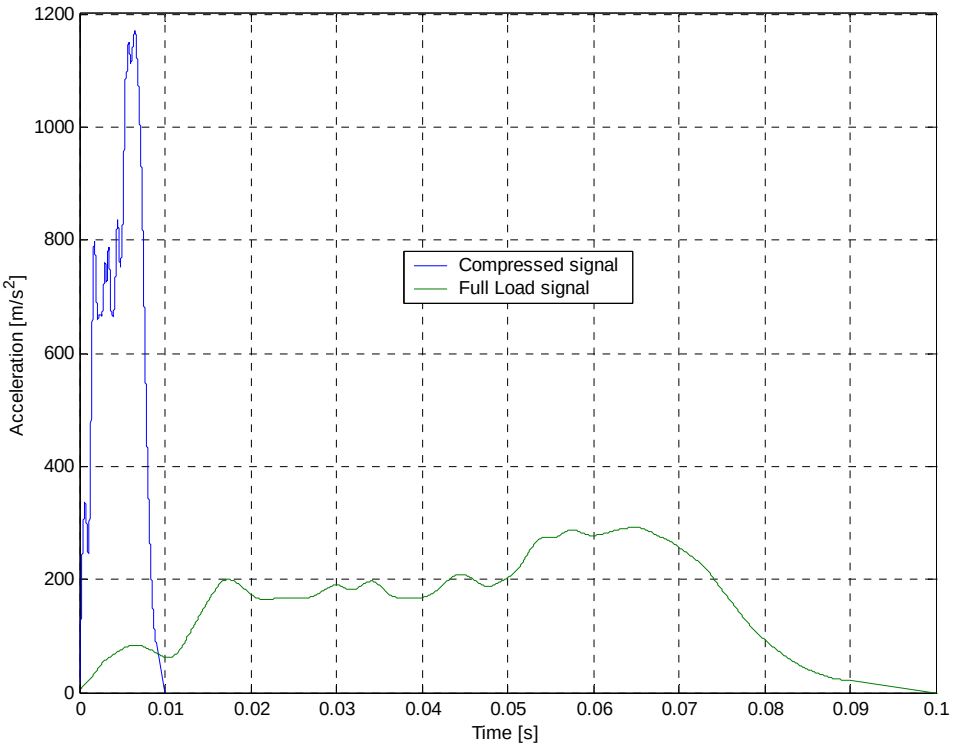

Figure 5.4: LS-DYNA load curves

5.3 Mathematical Optimisation

This section describes the methods used for the optimisation of the liquid container for impact. The section includes the definition of the optimisation problem, the setup of the automated optimisation process, and the results obtained.

5.3.1 Definition of Problem

As discussed in Chapter 2, the integrity of a liquid container is an important factor and can be an issue of law in the case of a vehicle's fuel tank. To demonstrate the integrity of the fuel tank as a constraint for numerical design optimisation, the maximum principal stress in the baffles of the liquid container will be monitored and considered violated if it exceeds a predefined maximum value. The objective of the problem will be to reduce the mass of baffles in the container without sacrificing their integrity as defined.

5.3.2 Problem Setup

Figure 5.5 shows a flow diagram for the cycle followed during the optimisation for impact problems. This method is applied in both analyses that are discussed later in this chapter.

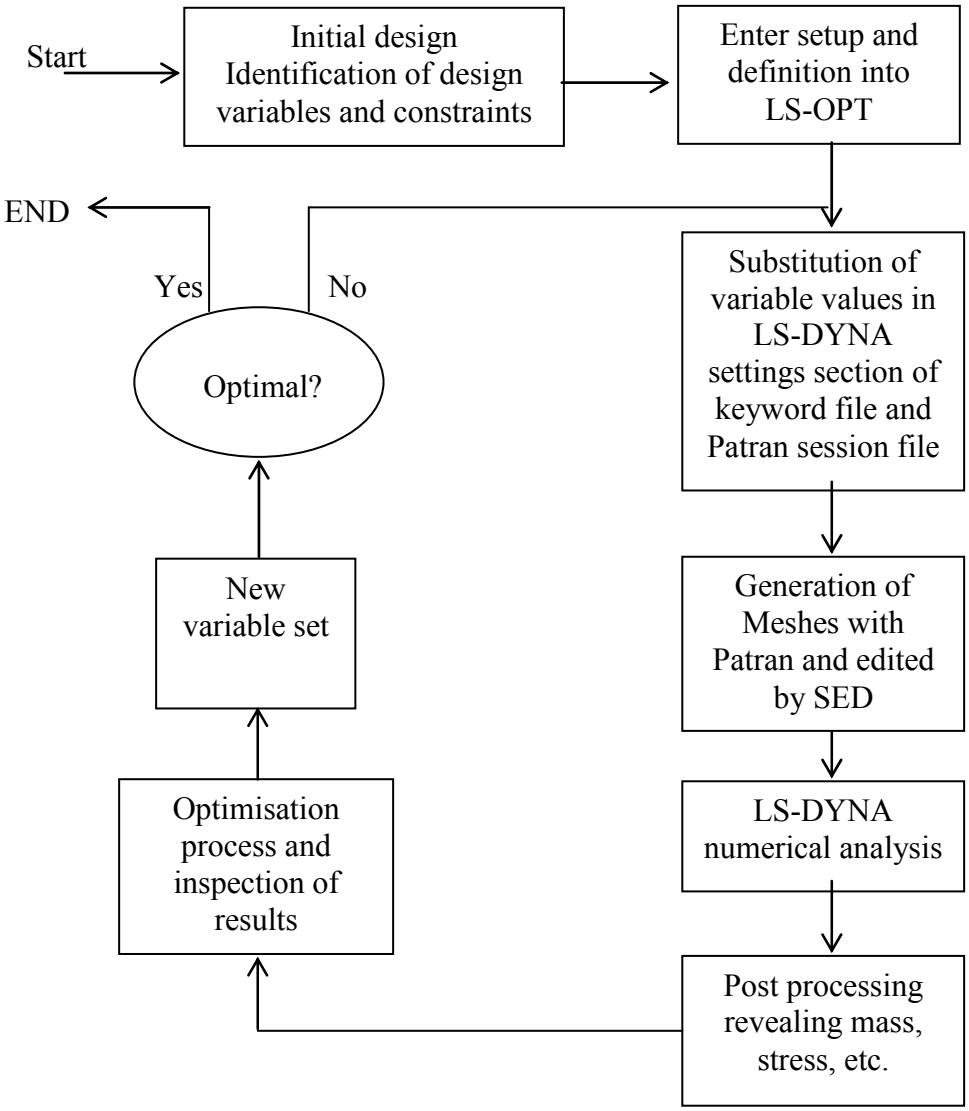

Figure 5.5: Flowchart for optimisation of impact problems

5.3.2.1 3D Geometry Optimisation Problem Definition

The 3D geometry optimisation was done using the Linear RSM method in LS-OPT (see Appendix V for LS-OPT command file). In accordance with Figure 5.1 above, the problem is defined as in Equation 5.1 below.

$$\textit{Variables } \mathbf{x} = [x_1, x_2, x_3]^T \tag{5.1}$$

x_1 = Hb = Baffle height

x_2 = ØD =Hole diameter

x_3 = Baffle thickness

Objective:

min f(**x**) = Baffle mass = volume * density

Subject to:

Inequality constraints-

$g_1(\mathbf{x})$ = Max Principal Stress in Baffle < 200e6 Pa

$$g_2(\mathbf{x}) = \frac{x_1}{2} - x_2 > 0.03$$

Side constraints-

$g_3(\mathbf{x})$: x_1 (Hb) (80;300)mm

$g_4(\mathbf{x})$: x_2 (ØD) (15;50)mm

$g_5(\mathbf{x})$: x_3 (Thickness) (1;10)mm

Constraints g_2 to g_5 are all geometrical constraints and ensure the feasibility of the proposed geometry. Inequality constraint g_1 enforces the integrity of the design by ensuring that the maximum principal stress does not exceed the yield strength of the material used for the baffles (200 MPa in this case).

5.3.2.2 2D Geometry Optimisation Problem Definition

The 2D "extruded" geometry optimisation was done using the Linear RSM method in LS-OPT (see Appendix W for LS-OPT command file) and took approximately 1.5 weeks on a 3GHz P4 Linux workstation for the number of iterations shown below. The topology represents a reduced version of that seen in Chapter 4, 2D container design 2. Side baffles are neglected for the impact analysis as very little strain is placed on their integrity. In accordance with Figure 5.2 above, Equation 5.2 below provides the problem definition.

$$\textit{Variables } \mathbf{x} = [x_1, x_2, x_3]^T \tag{5.2}$$

x_1 = MBC = Middle baffle centroid

x_2 = MBH =Middle baffle height

x_3 = Baffle thickness

Objective:

min f(**x**) = Baffle mass = volume * density

Subject to:

Inequality constraints-

$g_1(\mathbf{x})$ = Max Effective V-M Stress in Baffle < 200e6 Pa

$$g_2(\mathbf{x}) = \frac{x_1}{2} + x_2 < 0.34$$

$$g_3(\mathbf{x}) = x_2 - \frac{x_1}{2} > 0.02$$

Side constraints-

$g_4(\mathbf{x})$: x_1 (Hb) (40;320)mm

$g_5(\mathbf{x})$: x_2 (ØD) (60;320)mm

$g_6(\mathbf{x})$: x_3 (Thickness) (1;10)mm

Constraints g_2 to g_6 are all geometrical constraints and ensure the feasibility of the proposed geometry. Again, inequality constraint g_1 enforces the integrity of the design, but instead of maximum principal stress, the maximum effective Von-Mises stress is used. The discussion of results below explains the reason for this choice.

5.3.3 Optimisation Results

The following section provides the results of the optimisation analyses described in section 5.3.2 above. Results will include the improvement of the design w.r.t. its starting value as well as the progression of all the variables and responses during the optimisation process.

5.3.3.1 LS-OPT 3D Impact Case Optimisation

As stated before, this study involves a Linear RSM approach within the LS-OPT framework. Table 5.2 below provides the final results for this case. Figure 5.6 below illustrates the progress of the Linear RSM optimisation run. The optimisation required seven function evaluations per optimisation iteration with a total of 43 evaluations which took approximately 2 weeks to complete on a 3GHz P4 Linux workstation for the number of iterations shown below.

Table 5.2: Final Results for 3D impact case

	Starting value	Converged linear RSM result
Hb (x_1) [mm]	100	90
ØD (x_2) [mm]	25	15
Thickness (x_3) [mm]	2	3.83
Mass*10 f(x)	2.26	**4.04**
Max Stress (g_1) [MPa]	623	**186**

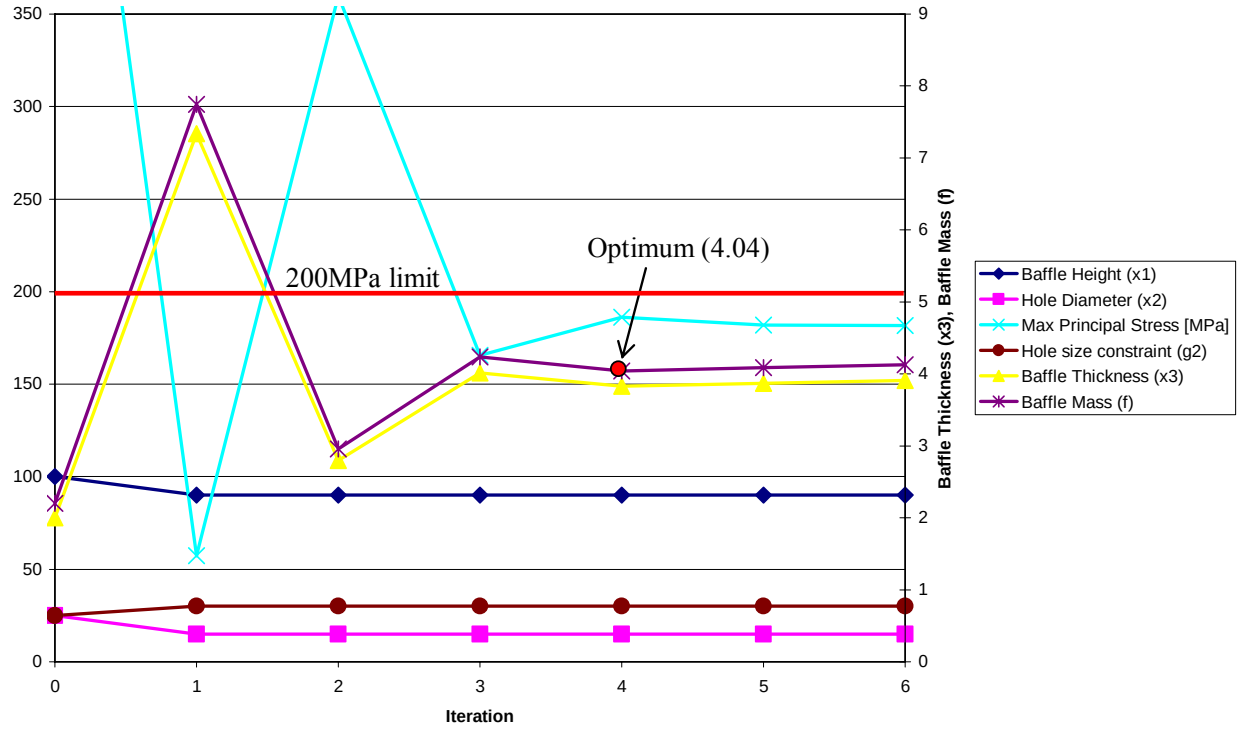

Figure 5.6: Optimisation history for 3D impact case

The first point of interest point is that the objective of mass has in fact increased with respect to the starting design. This is for no reason other than that the starting design violates the first inequality constraint of maximum principal stress by over 400 MPa. Although the first two variables of baffle height and hole diameter converge after the first iteration, the baffle thickness must establish sufficient magnitude to ensure structural integrity. The hole diameter and baffle height combine to achieve the smallest allowable frontal area for the baffle (as per constraint g_2 which restricts the hole from becoming too large relative to the baffle height). This intuitively reduces the level of inertial impact experienced by the baffle. This reduction is however insufficient and the baffle must be further strengthened by increasing its thickness from a starting value of 2mm to a final value of 3.83mm. Inequality constraint g_2 is active, but the limit of g_1 has not been attained. After further investigations it would seem that the principal stress method of establishing structural integrity does not perform as well as the maximum Von-Mises Stress method utilised in the 2D-extruded case of Section 5.3.3.2.

Figure 5.7 below provides an illustration of the 3D impact-case geometry with the variables corresponding to those for the optimum case. The image also provides contours of stress for a discrete moment, 0.008 seconds (Not necessarily peak stress), illustrating stress concentrations near the tank walls.

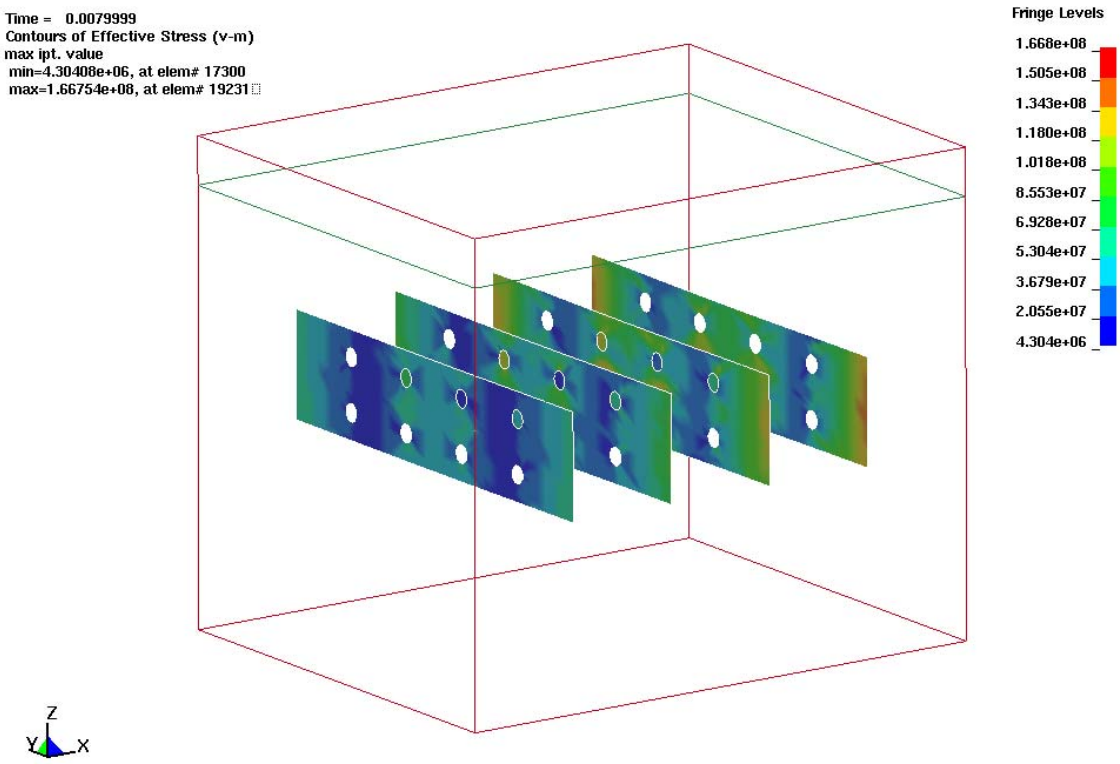

Figure 5.7: Optimum 3D impact-case geometry showing effective Von-Mises stress concentrations

5.3.3.2 Optimisation results for 2D "extruded" case

As stated before, this study involves a Linear RSM approach within the LS-OPT framework. Table 5.3 below provides the final results for this case. Figure 5.8 below illustrates the progress of the Linear RSM optimisation run. The optimisation required seven function evaluations per optimisation iteration with a total of 57 evaluations which took approximately 1.5 weeks to complete on a P4 3GHz Linux workstation.

Table 5.3: Final result for 2D "extruded" impact case

	Starting value	Converged linear RSM result
MBC (x_1) [mm]	100	113.6
MBH (x_2) [mm]	100	40
Thickness(x_3) [mm]	8	6.84
Mass*10 f(x)	30.1	**12.85**
Max Stress (g_1) [MPa]	153.8	198

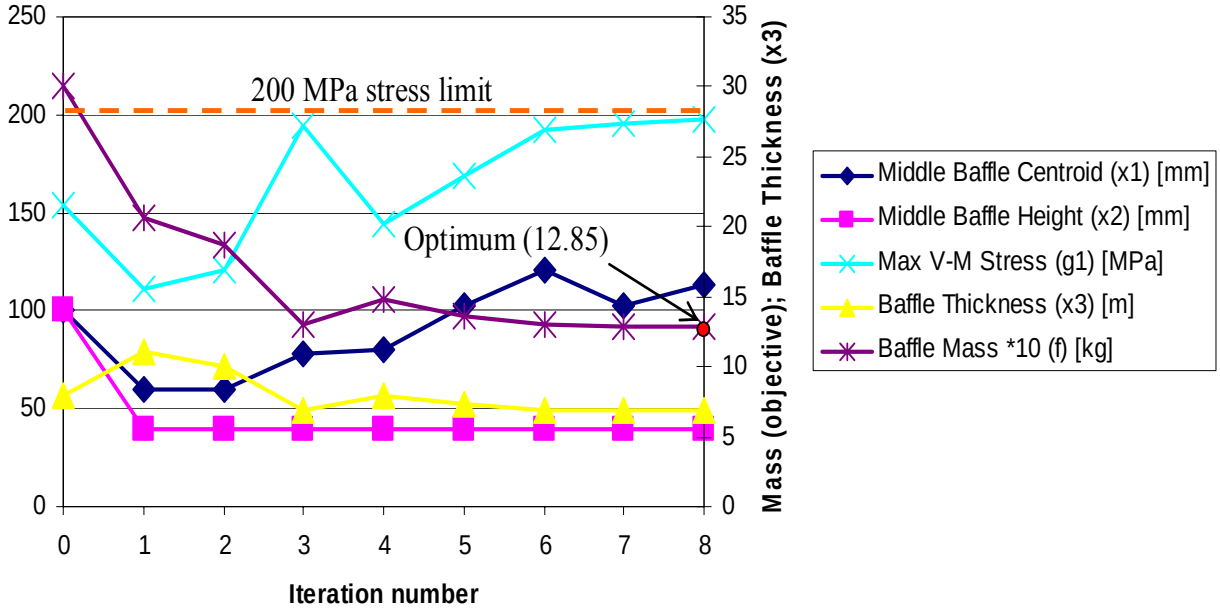

Figure 5.8: Optimisation history for 2D "extruded" impact case

This case provides a contrast to the previous case with an improvement in the objective function of 65%. This is because the maximum stress constraint is not violated but is in fact satisfied for the starting design. The baffle thickness is however significantly larger (6.84mm vs. 3.83mm). It is clear that the maximum Von-Mises effective stress is a stricter measure of stress than the maximum principal stress. It would furthermore seem that the maximum effective Von- Mises stress is a smoother and more reliable measure of the structural performance or integrity of the baffles.

During the optimisation process, the use of the Von- Mises stress demonstrated improved optimisation stability.

In terms of the impact event, the first two variables for baffle height and centroid location have moved to place the baffle as high as possible and make it as small as possible respectively. The explanation for this is firstly that again a smaller frontal area will absorb less of the inertia of the fluid and by being nearer the top of the container allows some of the deflected fluid to move more freely into the small space occupied by air near the top of the tank. The active constraints include the one that restricts the upward movement of the baffle (g_2) and the maximum stress in the tank (g_1).

Figure 5.9 below gives an illustration of the 2D "extruded" impact-case geometry with the variables corresponding to those for the optimum case. The image provides contours of stress for 0.01 seconds (Not necessarily peak stress), illustrating stress concentrations near the tank walls. Also note slightly higher concentrations near the lower half of the baffle indicating that the fluid near the free surface is free to move upward and therefore induce less impact energy onto the baffle in this region.

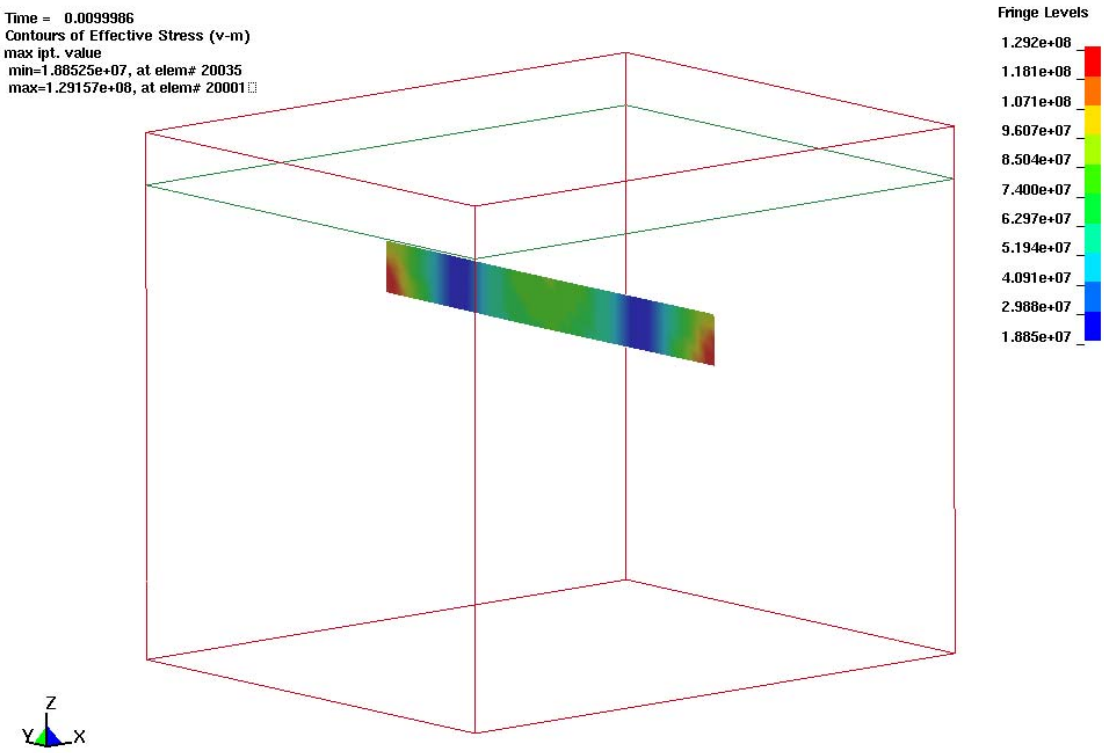

Figure 5.9: Optimum 2D "extruded" impact-case geometry showing stress concentrations

5.4 Conclusion

The results from this chapter illustrate the importance of the frontal area of the baffle with regards to the level of the impact energy it absorbs. Some insight into the impact event is provided however the section does show the need for multidisciplinary analysis. Since baffles are predominantly used for their ability to reduce sloshing, a large reduction in baffle size defeats the purpose of its inclusion in the impact design. The need for structural integrity does however not change and the combination of these challenges leads us to Chapter 6, multidisciplinary optimisation for both sloshing and impact.

CHAPTER 6: Multidisciplinary Design Optimisation for Sloshing and Impact

6.1 Introduction

This chapter covers the definition of a Multidisciplinary Design Optimisation (MDO) of liquid containers, considering both sloshing and impact criteria. The chapter covers the formulation and results of the MDO problem.

6.2 Definition of MDO Problem

The MDO problem of the liquid container is defined in such a way so as to consider the objectives discussed and utilised in the optimisation for sloshing section of the study (Chapter 4), as well as the objectives and criteria for integrity used during the optimisation for impact (Chapter 5). The aim is to attain a set of design variables that will provide both good sloshing performance and minimal use of material. The design must naturally also maintain structural integrity during an impact event.

The geometry considered is the same as those considered in sections 4.3.2.6 and 5.3.2.2 and is as shown in Figure 6.1 below.

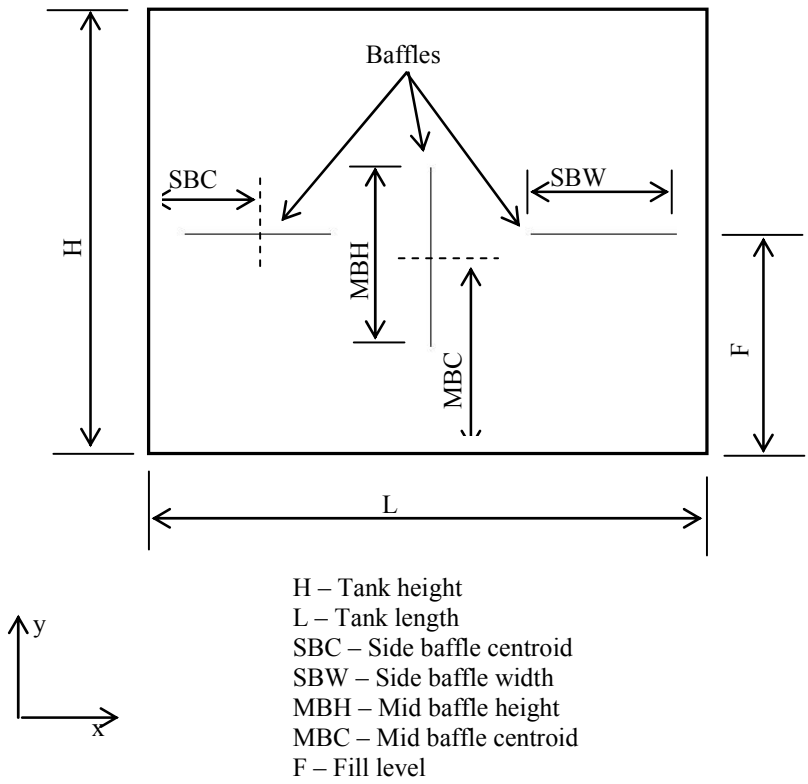

Figure 6.1: Geometry of container for MDO analysis

During the optimisation for sloshing analyses in Chapter 4, this geometry was referred to as design 2b, while in Chapter 5's optimisation for impact the identical geometry is entitled the 2D "extruded" geometry.

6.2.1 Problem Setup

All automated procedures are identical to those used during their respective analyses in Chapters 4 and 5. Both disciplines are now considered simultaneously and therefore require the separation of the variables into those that are shared and those that are considered by only one of the disciplines. The overall setup is best understood when examining it from a flowchart perspective as in Figure 6.2 below. Separate response surfaces are constructed for each discipline and combined in the manner prescribed by the weighting and scaling values (Equation 6.1). By separating the variables, the number of function evaluations required for each response surface is reduced [54]. Criteria for separation include variables that have no impact on the particular numerical solution as well as variables that have a minor or insignificant impact on

the numerical solution. This may be done in a number of ways. The first and simplest method is to use one's understanding of the specific phenomena in question and eliminating the variables that are known to have little significance. This can be backed up with a preceding sensitivity study and will provide a more economical, yet meaningful starting point for the optimisation procedure. The second method would be to utilise the information available from the response surface creation that is already part of the mathematical optimisation process. The ANOVA information described in Chapter 4 provides a quantitative measure of the significance of the various variables and can be used to discard less influential variables [54]. This second method will provide a way of reducing the computational expense of each optimisation iteration by discarding less significant variables. Only the first method is employed in this chapter.

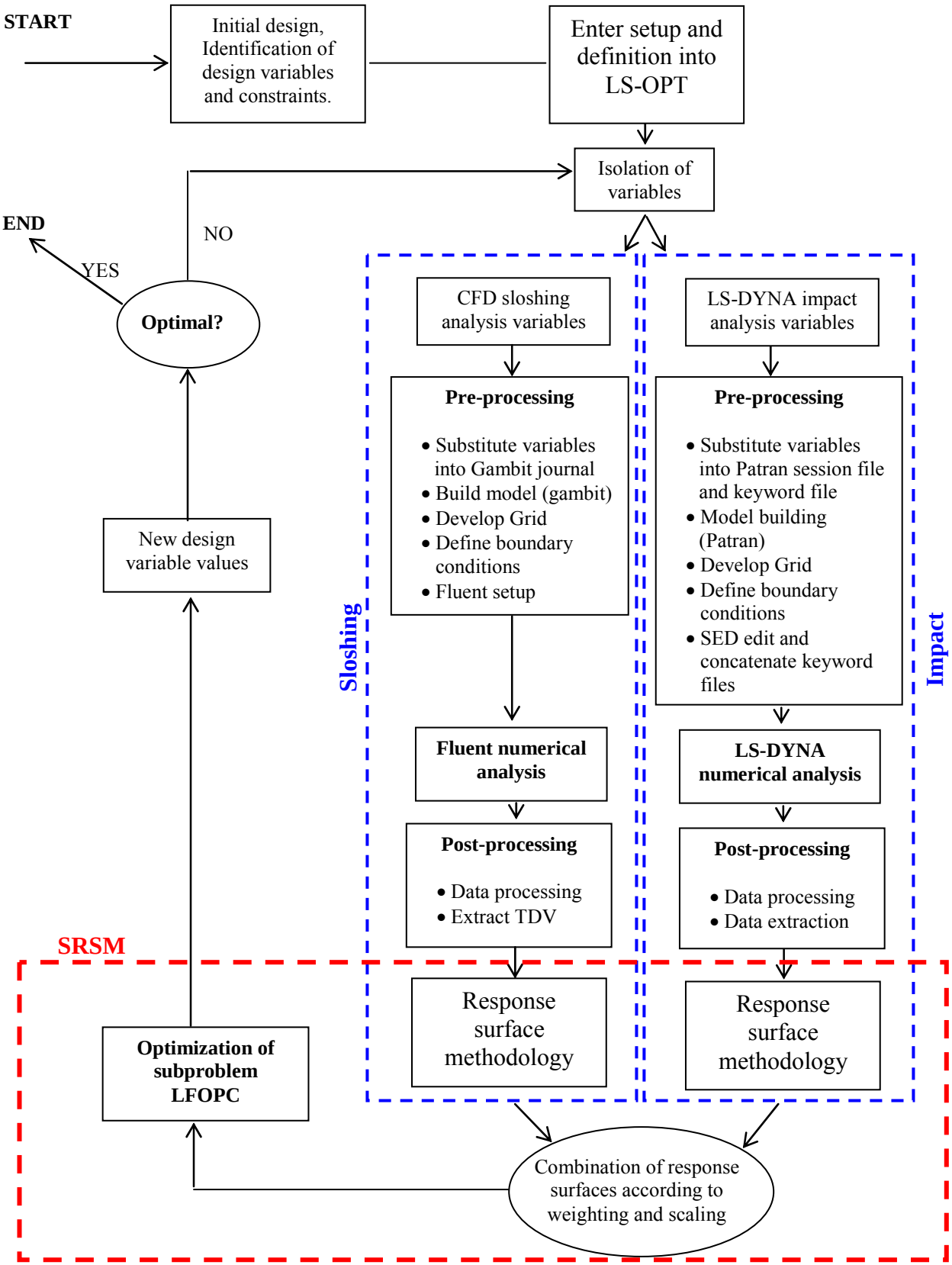

Figure 6.2: Flow diagram for MDO problem for sloshing and impact

6.2.2 Optimisation Problem Definition

The MDO was done using the Linear RSM method in LS-OPT (Command file included in Appendix X). Equation 6.1 below describes the optimisation problem definition, in accordance with the variables seen in Figure 6.1 above.

Multi objective: (6.1)

$$\min \ f(\mathbf{x}) = \sum_j \frac{f_j(x_j)\omega_j}{\alpha_j}$$

where:

$f_1(\mathbf{u})$ = Baffle mass = (Baffle volume) * density

$f_2(\mathbf{v})$ = TDV

weights :

$\omega_1 = 0.5$

$\omega_2 = 0.5$

scales :

$\alpha_1 = 0.1$

$\alpha_2 = 0.001$

Variables:

$\mathbf{x} = (\mathbf{u}, \mathbf{v}) = [x_1, x_2, x_3, x_4, x_5]^T$

x_1 = MBH = Middle baffle height $\{\in \mathbf{u} \ \& \ \mathbf{v}\}$

x_2 = MBC =Middle baffle centroid $\{\in \mathbf{u} \ \& \ \mathbf{v}\}$

x_3 = SBC = Side baffle centroid $\{\in \mathbf{v}\}$

x_4 = SBW = Side baffle width $\{\in \mathbf{v}\}$

x_5 = Baffle thickness $\{\in \mathbf{u}\}$

Subject to:

Inequality constraints-

$g_1(\mathbf{u})$ = Max V-M Stress in Baffle < 200e6 Pa

$g_2(\mathbf{v}) = - x_3 + 0.5*x_4 + 10\text{mm} < 0$

$g_3(\mathbf{v}) = x_3 + 0.5*x_4 - 190\text{mm} < 0$

$g_4(\mathbf{x}) = x_2 + 0.5*x_1 - 340\text{mm} < 0$

$g_5(\mathbf{x}) = - x_2 + 0.5*x_1 + 40\text{mm} < 0$

Side constraints-

$g_5(\mathbf{x})$: x_1 (MBH) (40;320)mm

$g_6(\mathbf{x})$: x_2 (MBC) (60;320)mm

$g_7(\mathbf{x})$: x_3 (SBC) (15;185)mm

$g_8(\mathbf{x})$: x_4 (SBW) (10;180)mm

$g_9(\mathbf{x})$: x_5 (Thickness) (1;15)mm

Constraints g_2 to g_5 are all geometrical constraints and ensure the feasibility of the proposed geometry. Inequality constraint g_1 enforces the integrity of the design by ensuring that the maximum Von-Mises stress does not exceed the yield strength of the material used for the baffles (200 MPa in this case).

As previously mentioned, the variables are separated into those relevant to each numerical analysis discipline. The thickness of the baffles is of no relevance to the CFD analysis since zero thickness is assumed for the baffles. This is justified by the fact that the relatively thin baffles will have little influence on the flow patterns associated with sloshing. The variables that define the side baffles are not used in the impact LS-DYNA analysis. The exclusion of the side baffle variables from the impact analysis is justified by the fact that peak stresses are seen in the middle baffle only, since the side baffles absorb very little of the fluid's inertia during impact. Considering that there is insufficient time during the impact analysis to develop any flow patterns, it is intuitive that the exclusion of the side baffles will not have much influence on the analysis results. By separating the variables, the total number of function evaluations per optimisation iteration is reduced from 20, i.e.,(10+10) for a fully shared scenario to 15, i.e.,(7+8) for the setup considered here. This will equate to

approximately 25% improvement in solution time per optimisation iteration that would have clear advantages in a design environment.

6.3 Optimisation Results

The multidisciplinary optimisation results in this section represent 13 optimisation iterations and a total of 5 partially shared variables. 3 variables are used in the impact analysis and 4 variables in the sloshing analysis. A total of 92 impact analysis function evaluations and 105 sloshing analysis function evaluations took approximately 3 weeks to solve on a 3GHz P4 Linux workstation. Figure 6.3 below illustrates the optimisation history of the objectives, variables and responses with respect to optimisation iteration number. The optimisation process exhibits reasonable convergence, and the final design represents an improved solution over the base design. The Von-Mises stress constraint is periodically active from the 9th optimisation iteration.

Table 6.1 below provides the starting an ending values for the variables, objectives and stress constraint.

Table 6.1: MDO analysis results

	Starting value	Final linear RSM result
MBH (x_1) [mm]	100	40
MBC (x_2) [mm]	100	263
SBC (x_3) [mm]	100	98.4
SBW(x_4) [mm]	100	10
Thickness(x_5) [mm]	8	7.46
Mass*10	30.1	**13.97**

$f_1(x)$		
TDV $f_2(x)*10^4$ [m.s]	49.17	**43.97**
Max Stress (g_1) [MPa]	153.8	198

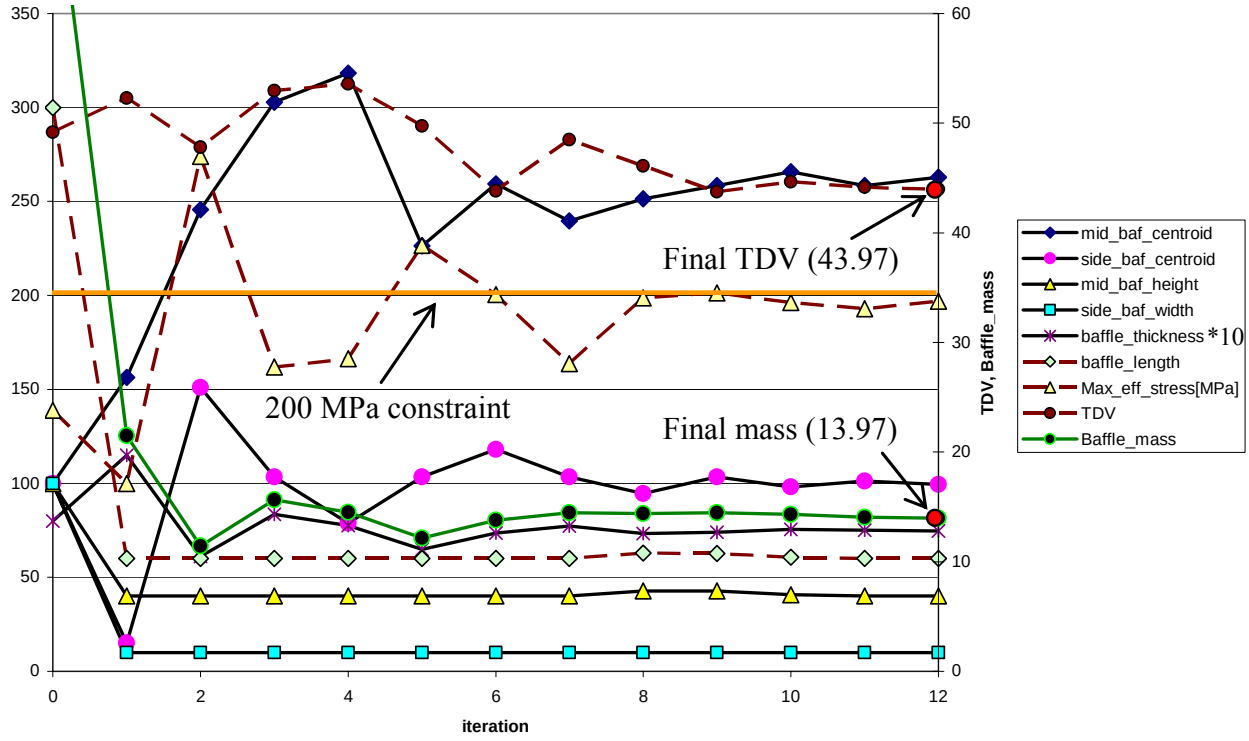

Figure 6.3: Multidisciplinary optimisation history

The results indicate an optimisation routine that has favoured the mass objective. As one would imagine, the baffle thickness is closely linked to the effective stress performance. The linear RSM used results in some oscillation of the design, but a converged solution is still obtained due to the sub-domain reduction scheme employed. The 50% weighting of the two objectives has still resulted in a greater improvement in the mass due to the relative difference between the starting design and a design that satisfies the stress constraint. In contrast, less design improvement is available for sloshing objective. This suggests that the MDO result is subject to the

initially chosen weighting between the objectives. This can be further extended to a design environment, where the setup may reflect a desired outcome. The mass of the container may come at a higher premium than the reduction of sloshing. More importantly, the methodology presented in this study allows for a simple method by which the engineer can manipulate the results to obtain a desirable result.

Figure 6.4 below illustrates the form of the final MDO design. Small side baffles suggest that the reduction in sloshing they provide is less than the reduction in mass that can be achieved by making them small. The position of the centre baffle is by no means coincidental. The centre baffle aligns itself with the fluid level (70% for sloshing) as this is the area where the horizontal velocities in the fluid are the highest. Furthermore, since the fluid level at the centre of the liquid container remains relatively constant, the centre baffle is active for most of the sloshing event.

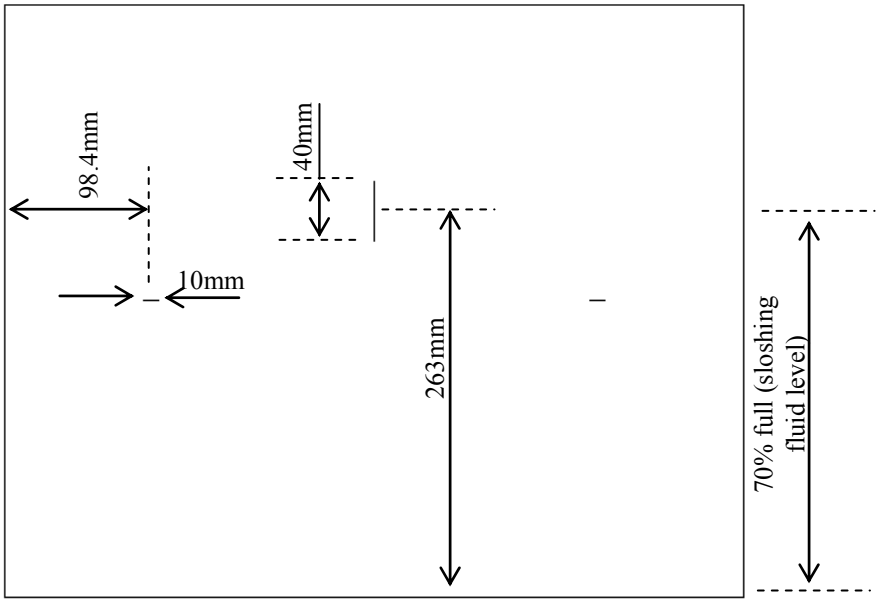

Figure 6.4: Final dimensions of MDO optimum design

6.4 Summary of Results

This section provides an overview of the results achieved for the various single and multidisciplinary optimisation studies on the same geometry. The three cases represent a sloshing only analysis, a mass and stress only analysis and the

multidisciplinary mass and sloshing analysis respectively. Table 6.2 below provides the results for the three cases. The two single discipline studies show what improvements can be achieved for baffle and/or TDV. Examining these results in conjunction with the case 3 (MDO) results, it is noted that a compromise between sloshing and baffle mass has been achieved. This indicates some success with regards to the setup of the multidisciplinary design optimisation routine.

Table 6.2: Summary of the optimisation results for the three optimisation scenarios

Case	Objective f	**Objective (start)**	**Objective (final)**	Design variables (start)	Design variables (final)	Constraints active
1 (case 6 in Chapter 4)	TDV	TDV = 49.17 [m.s]	TDV = **29.37** [m.s]	$\boldsymbol{x}_{slosh}$= (MBC,SBC,MBH, SBW) = (100,100,100,100)	$\boldsymbol{x}_{slosh}$= (MBC,SBC,MBH, SBW) = (162,78,244,136)	SB side, MB lower
2 (2D extruded case in Chapter 4)	Baffle mass	Mass = 30.1‡ [kg]	Mass = **12.85** [kg]	$\boldsymbol{x}_{impact}$= (MBC,MBH,Thick ness)= (100,100,8)	$\boldsymbol{x}_{impact}$= (114,40,6.84)	Maximum effective von Mises baffle stress = 198 MPa
3	0.5TDV + 0.5Baffle mass	TDV = 49.17 [m.s]; Mass = 74.88 [kg]	TDV = **43.97** [m.s]; Mass = **13.97** [kg]	$\boldsymbol{x}_{slosh+impact}$= (MBC,SBC,MBH, SBW,Thickness)= (100,100,100,100,8)	$\boldsymbol{x}_{slosh+impact}$ (263,98.4,40, 10,7.46)	Maximum effective von Mises baffle stress = 198MPa

The behaviour of MBC is sited as quite interesting in that at first glance this would appear counter intuitive, however, these values should be read in conjunction with the value for MBH (middle baffle height). For the sloshing only optimisation (Case 1), the middle baffle is very large and only the upper edge of the baffle is interacting with the free surface. This gives optimal sloshing performance but uses a lot of material. For the MDO case (Case 3) the upper surface is still interacting with the free surface but the baffle is very small (to reduce mass). The result is

‡ The starting mass for the impact only case is lower due to an assumed constant side-baffle width of 10mm since it is excluded from the analysis.

that the centroid of the baffle is high. Since sloshing is not a part of the impact analysis (Case 2), I do not believe the stresses to be very sensitive to its location. Figure 5.8 does however suggest that if further iterations were performed the location of the centroid would be higher. Therefore for the MDO case the lack of sensitivity of the stresses to MBC suggest that its location was determined by the sloshing discipline while the baffle's reduced size gave a lower mass.

6.5 Conclusion

This chapter illustrates the setup and results of the combining of the single disciplinary design optimisation techniques used in previous chapters. When considering sloshing only, the optimization algorithm employed effectively reduced the total deviation value used as an objective. When impact only was considered, the baffle mass was effectively reduced until the specified stress constraint was reached. The Multi-disciplinary Design Optimisation results, considering both sloshing and impact, show that a compromise could be found between sloshing behaviour and effective stresses in the baffles due to impact. Other formulations of the MDO problem may be considered, and the results will be highly dependent there on. The specific formulation will depend on the design engineer and results of interest.

CHAPTER 7: CONCLUSION AND FUTURE WORK

This dissertation documents the work covered during the study of numerical design methods in the liquid container design environment. The work covers as many aspects as possible, from analysis and experimental validation to fully automated multidisciplinary design optimisation. The conclusions made during this study are as follows.

Chapter 2 indicated the large array of tools available to an engineer in the liquid container design cycle. An overview of the work done to this point suggests that multidisciplinary combinations of these tools to consider both sloshing and impact would be relatively new work. The limits and boundaries selected for use with these design tools are in some cases governed by legal requirements, as with vehicle fuel tank design.

The chapter that follows covered the modelling of the sloshing phenomena inside a liquid container using Computational Fluid Dynamics. This section provided sufficient insight into the validity of the numerical models as well as some level of insight into the phenomena typical in liquid container sloshing. Discrepancies between the measured and simulated sloshing results were obtained and explained as more attributable to experimental inadequacies (filtration of acceleration content and low-frequency capability of the accelerometer) rather than to simulation (modelling) error. Significantly, within a design perspective, an improved numerical CFD model would seemingly translate to an improved physical design for sloshing.

Chapter 4 documented an extensive look at optimisation for sloshing techniques. The results of the optimisation runs indicate that response surface methods in conjunction with LS-OPT provide a robust and insightful method of numerical design optimisation of liquid containers for sloshing. The chapter illustrated some of the

statistical tools that are available for analysing the data available from an optimisation process.

Chapter 5 demonstrated the tools available in a finite element analysis environment to model a liquid container during an impact event and to establish container integrity. From an optimisation perspective, the results of an optimisation process that considers impact only give an as small as possible baffle. This however defeats the purpose of the baffle as a sloshing inhibitor and vindicates the need for a multidisciplinary optimisation process that considers both sloshing and impact.

As a combination of the best practice and most computationally economical design methods seen throughout the study, Chapter 6 presented the multidisciplinary design optimisation process that considers both sloshing and impact. The results of the process are encouraging, as a trade off is found between the requirements for an optimal design for both disciplines. The results suggest that the setup could be easily adapted to accommodate further geometries and circumstances. One of the observations made is that the result is largely influenced by the relative weighting or importance assigned to the respective disciplines. In addition, this implies that since a trade off exists, the desired result can be achieved by altering this discipline weighting.

The results achieved in this study pave the way for further studies in the field. The study may indeed be extended to three dimensions, both within the CFD model and the load curve. An example would be a liquid transporting vehicle performing a sudden turning manoeuvre. Full multi-body system dynamics may be included as a 3rd discipline (e.g., using ADAMS). Practical application of flow damping devices will in general need to accommodate full 3D free-surface motion. Another potential point of interest is the design and evaluation of moving baffles or other dynamic damping devices and the capabilities of CFD codes to handle multi-degree of freedom rigid bodies within the flow domain.

If computational resources exist, a full trade off curve would provide interesting inside into the influence of the weighting of the two disciplines in a multidisciplinary design optimisation process.

As this dissertation went to press, Fluent released an LES model that can work in conjunction with VOF. This will allow for the solution of acoustics and the quantification of sound pressure levels. This can be used at both the experimental verification level, comparing measured sound levels, and as a possible alternative objective.

The structural integrity analyses can be extended to the complete impact simulation of the liquid container, as prescribed by the safety standards. Recent advancements in the simulation of fluid-structure interaction allow for the simultaneous solution of a CFD and FEM solver while coupling the two methods with the transfer of pressure and deformations data (e.g., MPCCI). The merits of utilising the strengths of the two methods (CFD and FEM) in one coupled solution should be evaluated for improved accuracy.

Finally, this study successfully demonstrates the use of multidisciplinary analysis of liquid containers, but the processes illustrated could be applicable to any number of flow problems that invariably have structural design challenges included. Incorporating numerical optimisation with this multidisciplinary approach brings an added level of design cycle and time scale economy that is undoubtedly of benefit to any industrial design process.